

Capture of vacancies by extrinsic dislocation loops in silicon

S. B. Herner,^{a)} H.-J. Gossmann, F. H. Baumann, G. H. Gilmer, and D. C. Jacobson
Bell Laboratories, Lucent Technologies, Murray Hill, New Jersey 07974

K. S. Jones

Department of Materials Science and Engineering, University of Florida, Gainesville, Florida 32611

(Received 10 October 1997; accepted for publication 28 October 1997)

The capture of a flux of vacancies in Si by a band of extrinsic dislocation loops has been observed in Sb doping superlattices. Annealing Sb doping superlattices containing a band of dislocation loops in NH₃ results in an injection of vacancies, which enhances the diffusion of Sb spikes located between the surface and loop band. By extracting the diffusivity in the Sb spikes on either side of the loop band, we conclude that over 90% of the injected vacancies are captured by the loops.
© 1998 American Institute of Physics. [S0003-6951(98)00701-3]

It had been demonstrated that native point defects concentrations are the major factor influencing the diffusion of common substitutional dopants in silicon.¹ Extended defects in silicon can be clusters of point defects, such as extrinsic dislocation loops, which are composed of self-interstitials. Extended defects arise from several common processing steps in integrated circuit (IC) processing, and are typically metastable, growing, and dissolving under various different conditions. This metastability implies that they can be a source or a sink of native point defects. The interaction of point and extended defects is therefore of obvious interest as shrinking device size dictates stricter understanding and control over dopant diffusion in silicon. Many studies have shown that excess interstitials are effectively captured with little or no energy barrier by preexisting extrinsic dislocation loops in silicon under some conditions.² No experimental studies have been done of the capture efficiency of vacancies by dislocation loops in silicon.

In this letter we report on the capture of vacancies by a layer of preexisting extrinsic dislocation loops in Sb doping-superlattices. Antimony has been shown to diffuse by a vacancy-dominated mechanism in silicon. Therefore, the intrinsic diffusivity of Sb is directly proportional to the vacancy concentration in Si.³ Several processing steps used in IC processing can lead to a supersaturation of vacancies: MeV ion implantation,⁴ and the presence of either a silicon nitride (SiN_x),⁵ or titanium disilicide (TiSi₂)⁶ film on silicon. We study the capture of a flux of vacancies injected by a SiN_x film into a band of end-of-range (EOR) dislocation loops. The EOR loops arise from the agglomeration during annealing of excess self-interstitials from the ion implant.

We can estimate the capture probability of vacancies diffusing through the band of dislocation loops. If we assume that vacancies will annihilate only at the dislocation core and at any nearest neighbor site to the core, the fraction of atomic sites in the loop band that are annihilating is the ratio of the volume occupied by the annihilating sites to the total volume of the loop band

$$F = \frac{l\pi\lambda^2}{V}, \quad (1)$$

where $l = \sum_i 2\pi r_i$ (the total line length of the dislocations), r_i is the radius of each loop, λ is the capture radius, and V is the volume of the loop band. The number of hops that a vacancy would make in the region of the loop band if it were not annihilated is approximately given by

$$N = 6 \left(\frac{d}{\delta} \right)^2 \left(\frac{t}{d} \right), \quad (2)$$

where d is the distance to the deepest edge of the loop band, δ is the vacancy diffusion hop distance, and t is the thickness of the loop band. The term $(d/\delta)^2$ is an approximation for the average number of diffusion hops required for a net displacement d of the vacancy. The number of hops that a vacancy would take in the loop band that would result in annihilation is $P = FN$. For $P \geq 1$, the vacancy would have a high probability of being annihilated. For example, for $P = 20$, the vacancy would make 20 hops in the loop band where it would visit an annihilating site. For $P < 1$, there is only a fractional probability that the vacancy has visited an annihilating site. This assumes that there is no long range (long range being greater than one site distance) attractive force between vacancies and loops, and therefore is a lower limit on the actual annihilation probability.

Antimony doping-superlattices were grown by the low temperature molecular beam epitaxy technique.⁷ The epilayer consists of six Sb spikes, 10 nm wide, doped to a concentration of $6 \times 10^{19}/\text{cm}^3$, with peak centers spaced 100 nm apart, capped by 50 nm of Si, grown on p -type float zone Si (100) wafers ($\rho > 1000 \Omega \text{ cm}$). Four samples from this wafer received amorphizing implants at room temperature: two of 190 keV Si⁺ to a dose of $5 \times 10^{15}/\text{cm}^2$ and two of 190 keV Si⁺ to a dose of $1 \times 10^{16}/\text{cm}^2$. A fifth sample was annealed but not implanted. All of the samples received an 800 °C/60 min anneal in flowing Ar (1500 sccm, 99.95% purity) in a tube furnace to recrystallize the amorphized region and form the EOR loops. This anneal has been shown to run the transient enhanced diffusion (TED) from the implant to completion.⁸ One each of the implanted samples received a second anneal at 910 °C/60 min in NH₃ (1500 sccm, 99.9995% purity), while another set received a second anneal at 910 °C/60 min in Ar. The resulting test structure is shown in Fig. 1.

^{a)}Electronic mail: bherner@physics.bell-labs.com

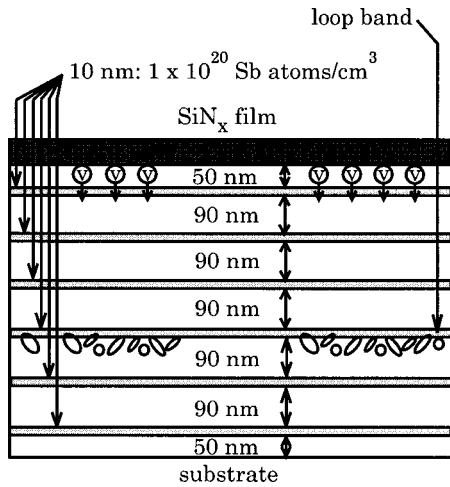


FIG. 1. Schematic of the test structure.

Samples for transmission electron microscopy (TEM) analysis were prepared by standard lapping and ion milling for cross section transmission electron microscopy (XTEM) or lapping and chemical etching for plan view transmission electron microscopy (PTEM) analysis. Samples were examined on either a JEOL 4000EX operating at 400 keV (PTEM) or a Phillips 420 operating at 120 keV (XTEM). Depth profiling was performed by secondary ion mass spectrometry (SIMS) using 3 keV Cs⁺ to sputter at a rate of 0.4 nm/s. Dopant diffusivities were extracted by analyzing each dopant spike separately as described in Ref. 9. Errors in the diffusivities have been estimated using a Monte Carlo approach.

All samples that were implanted had a band of EOR dislocation loops extending from 340 to 410 nm below the original surface [Fig. 2(a)]. The SiN_x film that formed on those samples annealed in NH₃ was 4 nm in thickness.¹⁰ The density of loops is shown, for example, in Fig. 2(b), for the high dose sample annealed in Ar both times. The sample has a high density of loops which lie on {111} planes, but the individual loops are distinct and do not form an extended network.¹¹ For both samples: $\lambda=4 \times 10^{-8}$ cm, $\delta=2.35 \times 10^{-8}$ cm, $t=7 \times 10^{-6}$ cm, $d=4.1 \times 10^{-5}$ cm, and $N=3.12 \times 10^6$. For the high dose (low dose) sample, $l=5.06 \times 10^5$ cm⁻¹ ($l=4.29 \times 10^5$ cm⁻¹), where l has been nor-

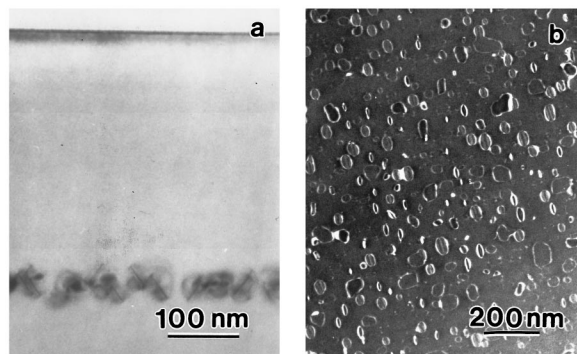


FIG. 2. (a) Bright field cross-section TEM micrograph of the sample implanted with 190 keV Si⁺ to 1×10^{16} /cm² and annealed 800 °C/60 min in Ar and 910 °C/60 min in NH₃; (b) Weak beam dark field plan view TEM micrograph of the sample implanted with 190 keV Si⁺ to 1×10^{16} /cm² and annealed 800 °C/60 min in Ar and 910 °C/60 min in Ar.

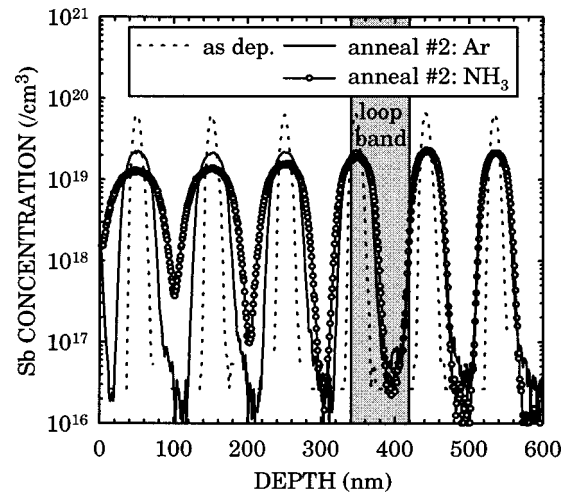


FIG. 3. SIMS depth profiles of the samples implanted with 190 keV Si⁺ to 1×10^{16} /cm² and annealed 800 °C/60 min in Ar (anneal No. 1) and 910 °C/60 min in either Ar or NH₃ (anneal No. 2).

malized to the area viewed in TEM, yielding $F=3.63 \times 10^{-4}$ (3.08×10^{-4}). This gives, for the high dose sample (low dose), $P=1130$ (961).

Typical secondary ion mass spectrometry (SIMS) depth profiles for implanted samples are shown in Fig. 3. Clearly, the sample that received a second anneal in NH₃ has enhanced diffusion of Sb in the shallow doping spikes between the film and the loop band. A previous measure of the vacancy diffusivity in Sb doping superlattices at 910 °C shows that the injected vacancies can easily reach the deepest doping spike with the given thermal budget.⁵ An extraction of the diffusivities of Sb in each of the doping spikes in all of the samples is shown in Fig. 4. The vacancies injected from the film are captured by the dislocation loop band in the samples implanted to either dose, in agreement with the prediction.

By taking the ratio of the average diffusivity in the first three spikes of samples in NH₃ to those annealed in Ar, we

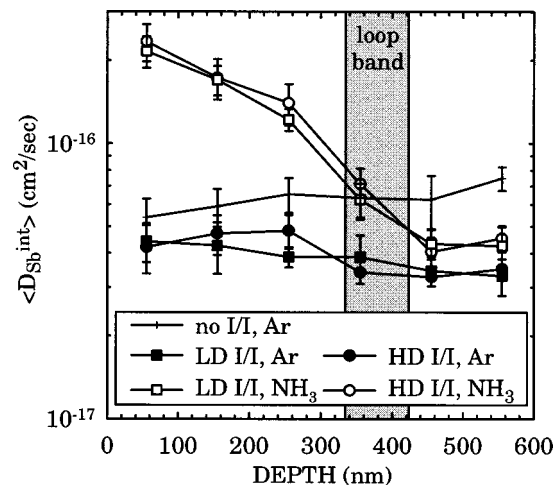


FIG. 4. Time-averaged total diffusivities of Sb in the spikes in each sample. LD I/I=190 keV, 5×10^{15} /cm² Si⁺ implant, HD I/I=190 keV 1×10^{16} /cm² Si⁺ implant; All samples were annealed 800 °C/60 min in Ar (anneal No. 1), and all were annealed 910 °C/60 min in either Ar or NH₃ (anneal No. 2). Annealing ambient No. 2 is shown after the implant condition.

obtain an estimate of the vacancy supersaturation at 910 °C, $\langle C_V \rangle / \langle C_V^* \rangle \sim 4$, where C_V is the concentration of vacancies, $\langle \rangle$ denotes time-averaged, and $*$ denotes equilibrium, where equilibrium is measured in the implanted samples annealed in Ar both times. This is in excellent agreement with a previous measurement of the vacancy supersaturation by Sb diffusivity⁵ and by monitoring the enhanced dissolution of extrinsic dislocation loops.¹⁰ The vacancy supersaturation in the two deepest spikes in the NH₃-annealed samples is $\langle C_V \rangle / \langle C_V^* \rangle \sim 1.25$, indicating that over 90% of the injected vacancies are captured by the loops. This confirms that the earlier measurement of vacancy supersaturation by measuring loop dissolution is accurate.¹⁰ We attribute the capture to the different strain states exerted by the defects: a negative strain in the case of vacancies and a positive one in the case of the extrinsic loops. Recombination at the loop band thus lowers the overall strain energy in the wafer. There is little difference between the samples implanted to different doses in their vacancy capturing efficiency. Jones *et al.*¹² have recently shown a reduced interstitial capture efficiency only in samples with much lower densities of dislocation loops than produced by the implants in this study. These conditions may result in lower vacancy capture probability as well, and these experiments should provide a measure of λ , the effective capture radius of a dislocation loop.

One other observation is pertinent with the data in Fig. 4. The implant and anneals in Ar have resulted in Sb-retarded diffusion in the ion-implanted samples compared to the sample that did not receive an implant, with a value of $\langle C_V \rangle / \langle C_V^* \rangle \sim 0.5$, where equilibrium here is measured in the sample that did not receive an implant. This vacancy undersaturation in the implanted sample appears in both the spikes that had been amorphized, as well as those that were not. This undersaturation could be due to interstitial-vacancy (*I-V*) recombination with the excess interstitials from the implant. If we count the interstitials bound by the loops (for details see Ref. 10), there are only $4 \times 10^{14}/\text{cm}^2$ interstitials

bound by the loops in the high fluence sample after being annealed in Ar both times. Therefore, only 4% of the $1 \times 10^{16}/\text{cm}^2$ implanted Si ions are in the loops, leaving plenty of free interstitials to recombine with vacancies.

In conclusion, we find that an EOR dislocation loop band effectively captures most of the vacancies injected by a thermally grown SiN_x film at 910 °C. We also observe a vacancy undersaturation in silicon that has been amorphized and regrown.

The authors would like to thank L. P. Pelaz for useful discussions, C. S. Rafferty for the provision of PROPHET, and R. Opila for his help with the experiments.

¹P. M. Fahey, P. B. Griffin, and J. D. Plummer, *Rev. Mod. Phys.* **61**, 289 (1989).

²D. J. Roth, R. Y. S. Huang, J. D. Plummer, and R. W. Dutton, *Appl. Phys. Lett.* **62**, 2498 (1993); H. Park, H. Robinson, K. S. Jones, and M. E. Law, *ibid.* **65**, 436 (1994); J. K. Listebarger, H. G. Robinson, K. S. Jones, M. E. Law, D. D. Sieloff, J. A. Slinkman, and T. O. Sedgwick, *J. Appl. Phys.* **78**, 2298 (1995); H. S. Chao, P. B. Griffin, and J. D. Plummer, *Appl. Phys. Lett.* **68**, 3570 (1996).

³P. Fahey, G. Barbuschia, M. Moslehi, and R. W. Dutton, *Appl. Phys. Lett.* **46**, 784 (1985).

⁴D. J. Eaglesham, T. E. Haynes, H.-J. Gossmann, D. C. Jacobson, P. A. Stolk, and J. M. Poate, *Appl. Phys. Lett.* **70**, 3281 (1997).

⁵T. K. Mogi, M. O. Thompson, H.-J. Gossmann, J. M. Poate, and H. S. Luftman, *Appl. Phys. Lett.* **69**, 1273 (1996).

⁶S. B. Herner, K. S. Jones, H.-J. Gossmann, J. M. Poate, and H. S. Luftman, *Appl. Phys. Lett.* **68**, 1687 (1996).

⁷H.-J. Gossmann, F. C. Unterwald, and H. S. Luftman, *J. Appl. Phys.* **73**, 8237 (1993).

⁸J. K. Listebarger, H. G. Robinson, K. S. Jones, M. E. Law, D. D. Sieloff, J. A. Slinkman, and T. O. Sedgwick, *J. Appl. Phys.* **78**, 2298 (1995).

⁹H.-J. Gossmann, A. M. Vredenberg, C. S. Rafferty, H. S. Luftman, F. C. Unterwald, D. C. Jacobson, T. Boone, and J. M. Poate, *J. Appl. Phys.* **74**, 3159 (1993).

¹⁰S. B. Herner, V. Krishnamoorthy, K. S. Jones, T. K. Mogi, M. O. Thompson, and H.-J. Gossmann, *J. Appl. Phys.* **81**, 7175 (1997).

¹¹K. S. Jones, S. Prussin, and E. R. Weber, *Appl. Phys. A: Solids Surf.* **45**, 1 (1988).

¹²K. S. Jones, K. Moller, J. Chen, M. Puga-Lambers, B. Freer, J. Berstein, and L. Rubin, *J. Appl. Phys.* **81**, 6051 (1997).